Mixing Associated with Sills in a Canyon on the Midocean Ridge Flank*

A. M. THURNHERR

Lamont-Doherty Earth Observatory of Columbia University, Palisades, New York

L. C. ST. LAURENT AND K. G. SPEER

Department of Oceanography, The Florida State University, Tallahassee, Florida

J. M. TOOLE AND J. R. LEDWELL

Woods Hole Oceanographic Institution, Woods Hole, Massachusetts

(Manuscript received 14 June 2004, in final form 9 February 2005)

ABSTRACT

To close the global overturning circulation, the production and sinking of dense water at high latitudes must be balanced elsewhere by buoyancy gain and upward vertical motion. Hydrographic and microstructure observations from the Brazil Basin in the South Atlantic Ocean indicate that most of the abyssal mixing there takes place on the topographically rough flank of the midocean ridge. In previous studies it has been suggested that the high level of abyssal mixing observed on the ridge flank is primarily caused by breaking internal waves forced by tidal currents. Here, the results from a detailed analysis of velocity, hydrographic, and microstructure data from a ridge-flank canyon are presented. Two-year-long current-meter records indicate that within the canyon there is a significant along-axial mean flow down the density gradient toward the ridge crest. Five hundred meters above the canyon floor the kinetic energy in the subinertial band exceeds that associated with the semidiurnal tides by approximately a factor of 2. The mean dissipation of kinetic energy inside the canyon exceeds that above the ridge-flank topography by approximately a factor of 5. The largest dissipation values were observed downstream of a narrow, 1000-m-high sill that extends across the full width of the canyon. Along the entire canyon, there is a strong association between the presence of sills and along-axial density gradients, while there is no similar association between the presence of depressions and density gradients. Together, these observations suggest that sill-related mixing contributes at least as much to the diapycnal buoyancy flux in the canyon as tidally forced internal-wave breaking, which is not expected to be associated preferentially with sills. While only ≈15% of the interfacial area between Antarctic Bottom Water and North Atlantic Deep Water in the Brazil Basin lie inside canyons, the available data suggest that approximately one-half of the diapycnal buoyancy fluxes take place there. In comparison, the region above the ridge-flank topography accounts for about one-third of the buoyancy fluxes. The apparent importance of sill-related processes for mixing in ridge-flank canyons is therefore of global significance, especially considering that such canyons occur on average every 50 km along 2/3 of the global midocean ridge system, and that sills partially block the canyon axes every few tens of kilometers.

1. Introduction

In the global overturning circulation, dense water is formed by ocean–ice–atmosphere interactions at high latitudes. The dense water masses sink to abyssal depths where they spread across all major ocean basins. To close the circulation, both buoyancy gain and upward vertical motion are required. The densest global water mass is Antarctic Bottom Water (AABW). Outside its formation regions on the Antarctic shelf, AABW is not in contact with the atmosphere. Therefore, it can only gain buoyancy by diapycnal mixing with less dense water and by geothermal heating. In the Brazil Basin, in the western subtropical South Atlantic Ocean, the contribution of geothermal heating to the AABW buoyancy budget is negligible (Hogg et al. 1982), implying that the observed buoyancy gain is pri-

* Lamont-Doherty Contribution Number 6771.

Corresponding author address: A. M. Thurnherr, Lamont-Doherty Earth Observatory of Columbia University, P.O. Box 1000, Palisades, NY 10964-1000.
E-mail: ant@ldeo.columbia.edu

marily caused by mechanical mixing with overlying North Atlantic Deep Water (NADW). Full-depth microstructure profiles (Polzin et al. 1997; St. Laurent et al. 2001), validated by a tracer-release experiment (Ledwell et al. 2000), indicate that most of the turbulent-energy dissipation in the Brazil Basin takes place on the rough flank of the Mid-Atlantic Ridge (MAR), where hydrographic observations indicate buoyancy loss in the NADW and buoyancy gain in the AABW (Thurnherr and Speer 2003). Morris et al. (2001) infer that the microstructure-derived diapycnal fluxes are sufficient to close the AABW heat budget in the Brazil Basin. Polzin et al. (1997) suggest that much of the enhanced mixing on the ridge flank is caused by breaking internal waves, because the high-dissipation observations commonly extend several hundreds of meters above the seabed. They furthermore assume that the tides dominate the deep velocity field in the Brazil Basin and hypothesize, therefore, that the enhanced mixing on the ridge flank is primarily tidally driven. This hypothesis is consistent with some evidence for a spring–neap modulation in the dissipation data (Ledwell et al. 2000; St. Laurent et al. 2001).

As is the case for all slow-spreading midocean ridges, the flanks of the MAR are cross-cut by deep canyons or valleys, which are the off-axes traces of transform faults (in which case the canyons are called fracture zones) and of second-order (nontransform) discontinuities (Tucholke and Lin 1994). In their analysis of the ridge-flank topography and hydrography in the tropical and subtropical South Atlantic, where the MAR accounts for more than one-half of the seabed area, Thurnherr and Speer (2003) find that the cross-flank canyons are typically 500–1000 m deep and spaced approximately every 60 km along the ridge flank. Within most of the canyons there are horizontal density gradients directed away from the ridge axis, that is, with the density decreasing toward the MAR crest. In cross-ridge hydrographic sections [e.g., in the World Ocean Circulation Experiment (WOCE) sections A08–A10], the along-canyon density gradients manifest themselves as isopycnal surfaces sloping down and intersecting the ridge flanks. Within the canyons meridional flows are blocked, implying that in the absence of external forcing the cross-flank pressure gradients drive up-valley flows down the density gradients toward the MAR crest (Thurnherr and Speer 2003). To achieve a steady state in such settings, the along-valley advection of buoyancy must be balanced by diapycnal mixing (St. Laurent et al. 2001; Thurnherr et al. 2002).

To extrapolate the dissipation data from the Brazil Basin to larger scales (e.g., Morris et al. 2001; St. Laurent et al. 2002), and to include the effects of spatially varying diapycnal mixing in numerical models (e.g., Huang and Jin 2002; Simmons et al. 2004), the mixing must be parameterized. Current parameterizations are primarily based on local topographic variance (roughness), without explicitly accounting for the presence of canyons. On the other hand, St. Laurent et al. (2001) classify the available microstructure profiles from the South Atlantic according to topographic setting and find that the observed dissipation in the ridge-flank canyons (including the slopes of the lateral canyon walls) is, on average, 2–3 times the dissipation over the crests of the lateral canyon walls. If this difference is significant, roughness-based parameterizations cannot be expected to be valid both in regions with and without canyons.

The first microstructure survey in the Brazil Basin revealed downward-increasing dissipation on the rough flank of the MAR, implying a buoyancy loss of the abyssal waters. This observation led Polzin et al. (1997) to speculate that the buoyancy gain required to close the AABW heat budget takes place in the deep ridge-flank canyons, and they report some evidence for a downward-decreasing trend in the dissipation below the peaks of the local bathymetry (i.e., inside the canyons). Subsequent dissipation observations do not support this assertion, however (St. Laurent et al. 2001). Interpretation of the dissipation measurements from the canyons is complicated by the fact that the profiles were not taken at random locations. In particular, the dissipation stations occupied on the ridge flank in 1997 coincided with the stations of a tracer survey (Ledwell et al. 2000). To sample the tracer cloud as completely as possible, the station positions were chosen near local depth maxima in the canyons. Therefore, there is some uncertainty as to the representativeness of the available dissipation data, especially considering also the observations from another abyssal valley, which indicate that diapycnal mixing can be greatly enhanced in the vicinity of topographic obstacles (sills) in the path of a mean along-valley flow (Thurnherr and Richards 2001; Thurnherr et al. 2002).

Here, we present the results from a detailed analysis of velocity, hydrographic, and microstructure data from a canyon on the western flank of the MAR near 22°S. In section 2, velocity observations from the canyon and from the overlying water-column are presented. Current-meter records confirm the heat-budget-derived inference of along-canyon flow down the density gradient toward the MAR crest (St. Laurent et al. 2001), although the observed velocities are several times larger than expected. Spectral decomposition furthermore reveals that the subinertial contributions to the kinetic energy at middepth in the canyon exceed the tidal con-

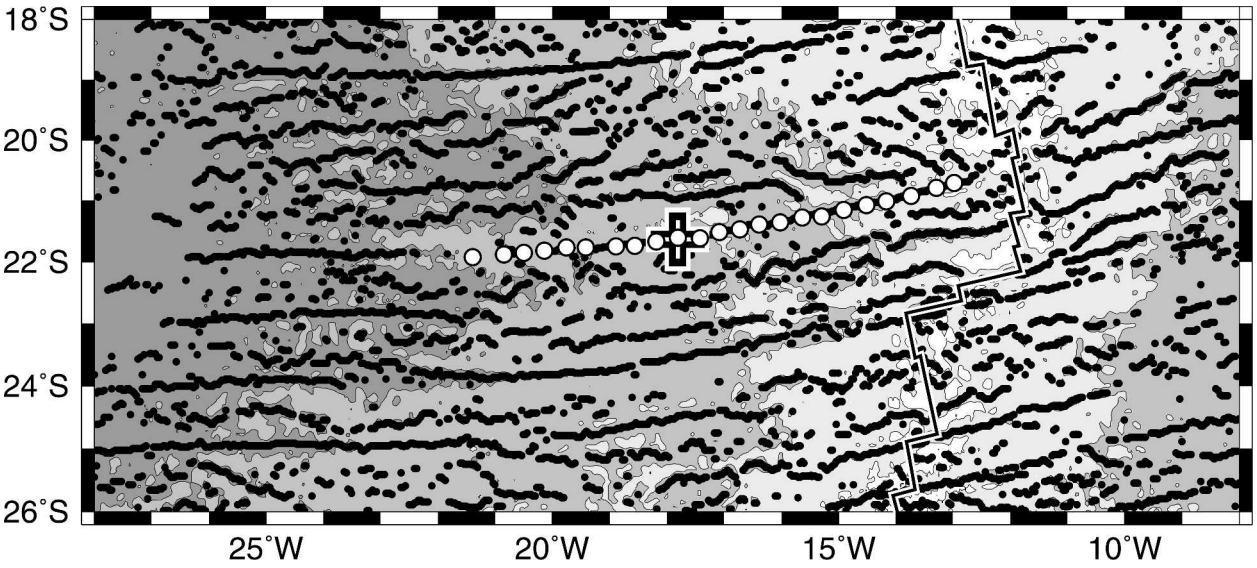

FIG. 1. Ridge-flank topography (Smith and Sandwell 1997, version 8.2), microstructure stations (bullets), and current-meter mooring (cross) in a canyon on the western flank of the MAR in the South Atlantic; the microstructure stations are a subset of the data analyzed by St. Laurent et al. (2001). Topographic contours are plotted at 3000, 4000, and 5000 m; black dots show meridional depth maxima primarily associated with cross-flank canyons (Thurnherr and Speer 2003); the ridge axis (Müller et al. 1997) is marked with a solid line.

tributions. In section 3 the mixing in the canyon is analyzed in detail. Because of expected high levels of intermittency the along-canyon distribution of mixing is primarily diagnosed from horizontal along-axial density gradients, rather than from dissipation data. Our analysis reveals that the mixing within the canyon takes place primarily near cross-canyon sills. Taken together (section 4), the observations suggest that (i) overflow-related processes in ridge-flank canyons may be at least as important for the abyssal buoyancy budget in the Brazil Basin as breaking internal tides, (ii) available dissipation data from the Brazil Basin are probably biased low because they were collected away from the regions where the horizontal density gradients imply the strongest diapycnal buoyancy fluxes, and (iii) geophysical considerations suggest cross-sill flows in ridge-flank canyons to be of global significance for the abyssal buoyancy budget.

2. Hydrography and flow in a ridge-flank canyon

In 1997, a hydrographic and microstructure survey was carried out along the axis of the same ridge-flank canyon in the Brazil Basin near 22°S (Fig. 1) where artificial tracer had been released in 1996 (Ledwell et al. 2000). The canyon (trending ≈80° true) intersects the ridge flank perpendicular to the crest and extends from the bottom of the Brazil Basin below 5500 m near 26°W to the MAR crest near 12°W, where any connection with the eastern basin is blocked below 3000 m. The mean horizontal near-bottom along-axial density gradient in the canyon is $\approx 10^{-7}$ kg m^{-3} m^{-1} (Thurnherr and Speer 2003), surprisingly similar to the 0.9 (± 0.2) $\times 10^{-7}$ kg m^{-3} m^{-1} observed in two connected rift-valley segments in the North Atlantic (Thurnherr et al. 2002).

The velocity field inside and above the ridge-flank canyon was measured using eight current meters deployed on a single mooring that was anchored in a depression in the canyon floor near 17°45′W (cross in Fig. 1; Fig. 2). [The ubiquitous cross-canyon topographic structures apparent in Fig. 2 are known as abyssal hills. They are intrinsically associated with seafloor spreading, although their formation is not understood in detail—e.g., Goff et al. (1995)]. The instruments recorded velocities at half-hourly intervals for a period slightly longer than 2 yr. Six of the current meters were grouped in pairs (25-m vertical separation) near 3000 m (instruments 1 and 2, ≈1000 m above the ridge-flank topography), near 4000 m (instruments 3 and 4, at the level of the adjacent canyon-wall crests), and near 4650 m (instruments 5 and 6, ≈500 m above the seabed); two additional instruments were placed closer to the seabed near 4875 m (instrument 7) and 5025 m (instrument 8). No valid direction data were recovered from instrument 4. Because of problems with the tape of instrument 8, no data were recorded 24% of the time (the gaps typically occur 1–2 times per day and last 1–6 h); the data from this instrument were not used in our analysis.

Over the 2 yr of sampling, mean up-canyon flow

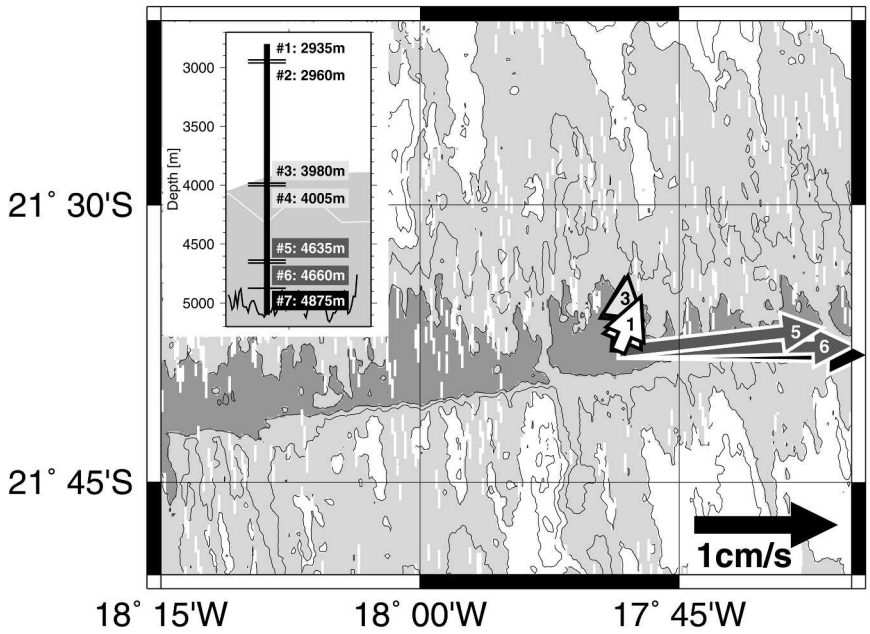

FIG. 2. (main) Multibeam topography near the current-meter mooring and record-mean velocities (arrows); the topography below 4500 m is shaded; dark gray is used below 5000 m; contour interval is 250 m; a subset of the arrow heads is labeled with the corresponding instrument numbers. (inset) Side view (looking north) of the mooring in the topographic context; lateral canyon walls are shaded (see Fig. 5 for details); labels indicate instrument numbers and depths.

down the density gradient was recorded by all current meters below the level of the adjacent canyon-wall crests (instruments 5–7). The observed mean speeds inside the canyon are 1.5–1.8 $\times 10^{-2}$ m s^{-1}; the corresponding uncertainties (standard errors of the means), estimated using the integral time scales of the records, low-pass filtered to remove fluctuations with periods less than a day, are 1.1–1.5 $\times 10^{-2}$ m s^{-1}. At and above the level of the canyon-wall crests (instruments 1–4) the record means are primarily northward, with speeds of 0.4–0.5 $\times 10^{-2}$ m s^{-1}. The corresponding uncertainties of 0.9–1.3 $\times 10^{-2}$ m s^{-1} imply that the northward record means of the upper instruments are not significantly different from zero. Lagrangian mean velocity estimates about these upper levels (from neutrally buoyant floats and from the displacement of the center of mass of a tracer cloud) also indicate weak flow (in both cases directed south to southwestward; Thurnherr and Speer 2003).

In contrast to the situation above the topography, the eastward mean flow in the canyon (instruments 5–7) is significantly different from zero. Without information on the cross-canyon structure of the flow field any estimate of along-canyon transport must remain tenuous. The qualitative consistency between the current-meter data and the up-canyon flow inferred from a heat budget (St. Laurent et al. 2001), as well as the alignment of the mean flow with the canyon axis imply, however, that at least the direction of the mean flow recorded by the current meters in the canyon is representative. In terms of magnitude, neither the possibility that the true cross-canyon averaged flow is stronger nor that it is weaker than the flow recorded by the current meters can be discounted. On one hand, lateral friction can retard the flow near the (heavily corrugated) canyon walls, implying that the current-meter velocities may be higher than the cross-canyon mean. On the other hand, rotation is expected to cause the up-canyon flow to be a boundary current, presumably banked up against the northern canyon wall, in which case the current-meter velocities would likely be an underestimate of the cross-canyon averaged mean flow.

The low-frequency currents at the depth of the canyon-wall crests (instruments 3–4) are similar to those 1000 m above the topography (instruments 1–2), whereas the flow within the canyon (instruments 5–7) appears essentially decoupled from the overlying water column (Fig. 3). The velocities near 3000 and 4000 m (instruments 1–4) are characterized by quasi-periodic oscillations with periods of several months, amplitudes of $\approx 2 \times 10^{-2}$ m s^{-1}, and clockwise (in time) rotating velocity vectors. There does not appear to be any preferred direction of the flow, consistent with the inference that the 2-yr mean velocities at 3000 and 4000 m

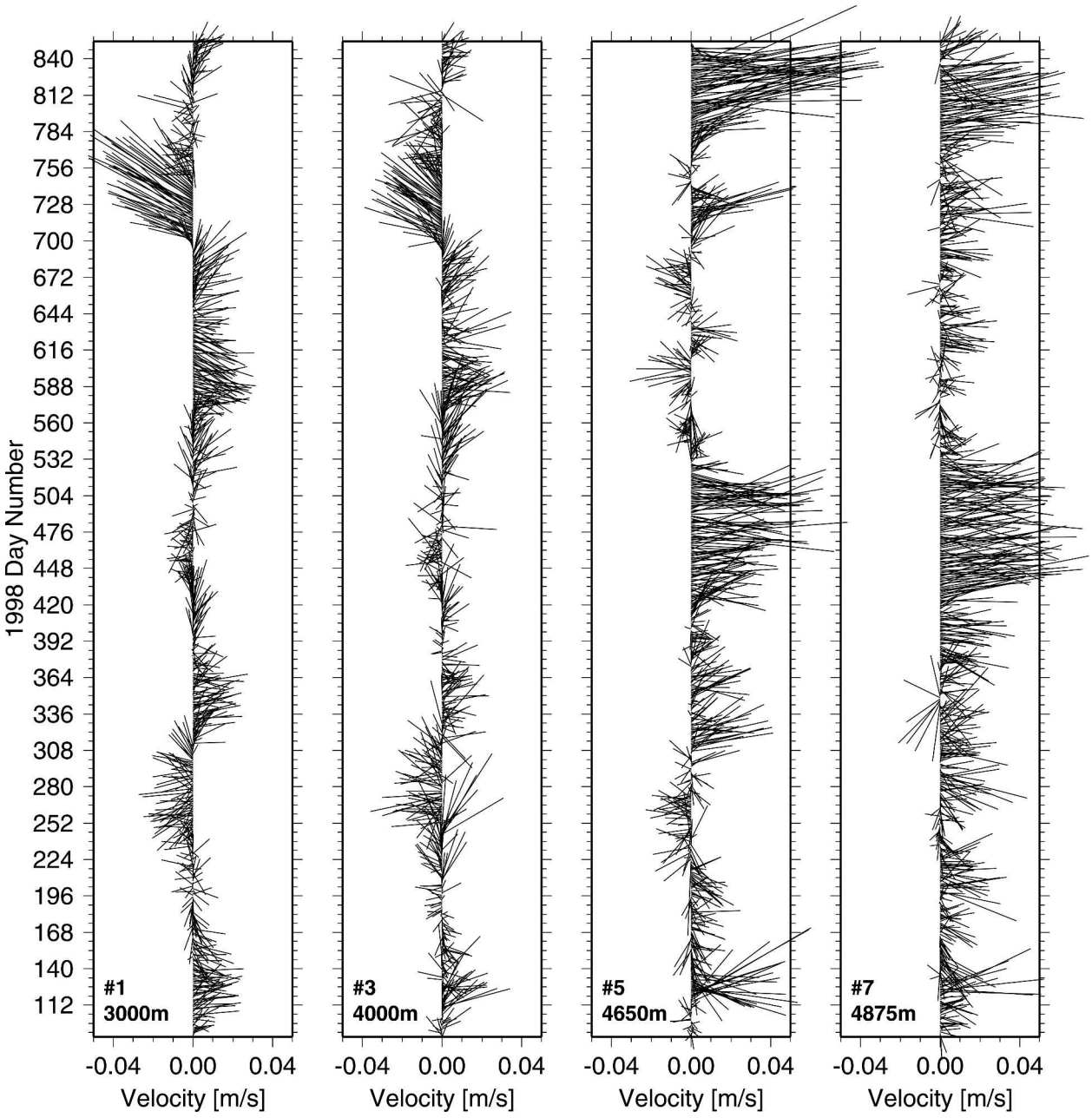

FIG. 3. Daily averaged current-meter velocities above the topography (instrument 1), at the level of the canyon-wall crests (instrument 3), and inside the canyon 500 m above the seabed (instrument 5) and 250 m above the seabed (instrument 7); only the records from the upper instruments of each pair are shown; north is up; the time axis is labeled every 28 days.

are not significantly different from zero. In contrast, the daily averaged velocities inside the canyon (instruments 5–7) are preferentially to the east. At these levels there is significant energy at low frequencies as well, but the fluctuations are less regular and stronger than those above the topography. The daily averaged up-canyon velocity peaks at >0.1 m s^{-1} at 4650 m on day 805. While the preferred flow direction in the canyon is toward the crest of the MAR, there are periods of daily averaged down-canyon flow. Two hundred fifty meters above the seabed (station 7), these down-canyon velocity pulses generally last only a few days. Without any information on the cross-canyon structure of the flow field it is unclear whether these episodes of down-canyon velocities are associated with down-canyon transports, or whether they are signatures of local recirculations.

The daily averaged velocities shown in Fig. 3 indicate

significant low-frequency energy in the velocity field at all levels. To compare the contributions from different frequency bands, velocity spectra were calculated. The linear presentation used in Fig. 4 ensures that the area underneath each curve is proportional to the kinetic energy per unit mass. (In contrast to variance-preserving spectra plotted in semilog form, the linear scaling of the frequency axis allows the energy associated with the mean flow to be included.) At 3000 and 4000 m (instruments 1–4), the largest velocities are associated with the semidiurnal tides, which account for 40%–45% of the total kinetic energy. The near-inertial band provides the next-largest contribution, accounting for 25%–35% of the total at and above the level of the canyon-wall crests. In addition to the inertial waves this band contains significant energy at a tidal-inertial interaction frequency. The low-frequency band (including the record mean flow) accounts for most of the remainder at 3000 m (instruments 1–2) but only for about half at 4000 m (instruments 3–4), the rest being provided by high-frequency motions in the internal wave band (not shown). Below the level of the adjacent canyon-wall crests at depths >4000 m the energy partition is different: At 4650 m (instruments 5–6) the contribution from the semidiurnal tide is reduced to 26% of the total while the low-frequencies account for 48%. The near-inertial velocities are similar to those at 4000 m, accounting for 19% of the total kinetic energy at 4650 m. 250 m above the seabed (instrument 7) the near-inertial band is largely suppressed, while the semidiurnal tide and the low frequencies account for 50% and 40% of the total kinetic energy, respectively.

3. Diapycnal mixing in the canyon

In their analysis of the available microstructure data from the Brazil Basin, St. Laurent et al. (2001) find that the near-seabed dissipation in ridge-flank canyons is 2–3 times the near-seabed dissipation above canyon-wall crests. The largest values were observed over the lateral canyon slopes—that is, at intermediate depths between the peaks of the canyon walls and the axial depth maxima. If the current-meter data shown in section 2 are representative, the largest dissipations therefore occur where the low-frequency band is most energetic and where the semidiurnal tides are weakest. In the microstructure data from the canyon analyzed here, 83% of the total dissipation below 2000 m takes place below the lateral canyon-wall crests (Fig. 5). A single profile (station 23) accounts for 22% of the observed dissipation in the canyon, suggesting that the mixing was undersampled. Even after removing this station from the dataset, mixing in the canyon accounts for 80% of the (now reduced) total. (The same percentages ±1% result when either the lower or the upper of the two canyon walls are used to partition the dissipation data.) While mixing over the MAR flank is enhanced throughout most of the water column (Polzin et al. 1997), the bulk of the diapycnal buoyancy fluxes (which are proportional to the dissipation of turbulent kinetic energy, if the usual assumption of a constant mixing efficiency is made) takes place within the topographic envelope of the ridge flank.

The highest depth-averaged energy dissipation in the canyon was observed on station 23. Approximately 10 km upstream (west) of this station the along-axial flow must cross a narrow sill that rises nearly 1000 m above the canyon floor and spans its entire width (Fig. 6). Most of the dissipation on station 23 occurs below the sill depth (Fig. 5). While the association of high dissipation with a nearby sill is suggestive, it is the only such association in the entire canyon. We reiterate, however, that all microstructure profiles in the canyon were taken near local depth maxima—that is, away from the immediate vicinity of sills (section 1).

In contrast to the microstructure observations, which provide temporal and spatial snapshots of the mixing intensity (which is assumed to be highly intermittent), along-axial density gradients are representative of the time- and space-integrated effects of mixing (Thurnherr and Speer 2003). To elucidate the along-canyon distribution of mixing, horizontal density gradients were calculated from 50-dbar-averaged hydrographic profiles at the sill depths (blocking depths) between each station pair. In regions where no high-resolution topographic data are available (stations 3–6 and 27–28; Fig. 5), and where the blocking depths are therefore not known, the density gradients were calculated at the bottom depths of the shallower of the two stations in each pair. The density-gradient uncertainty due to temporal variability was estimated from a repeat station occupied six times in two weeks in 1996 (Thurnherr and Speer 2003), yielding a value of $\approx 5 \times 10^{-8}$ kg m^{-1}, one-half of the thickness of an individual density-gradient block in Fig. 5. Along the canyon the density decreases monotonically toward the crest of the MAR. (The eastward density increase between stations 6 and 7 is not significantly different from zero.)

The near-bottom horizontal density gradient between stations 23 and 24, where the topography above 4000 m is not blocked by any sill, is 2.4×10^{-8} kg m^{-3} m^{-1}, approximately 1/20 of the density gradient across the sill between stations 22 and 23 (4.7×10^{-7} kg m^{-3} m^{-1}; Fig. 5). This difference is nearly 10 times larger than the uncertainty due to temporal variability, that is, it is highly significant. There are other regions in the canyon where consecutive station pairs are associated

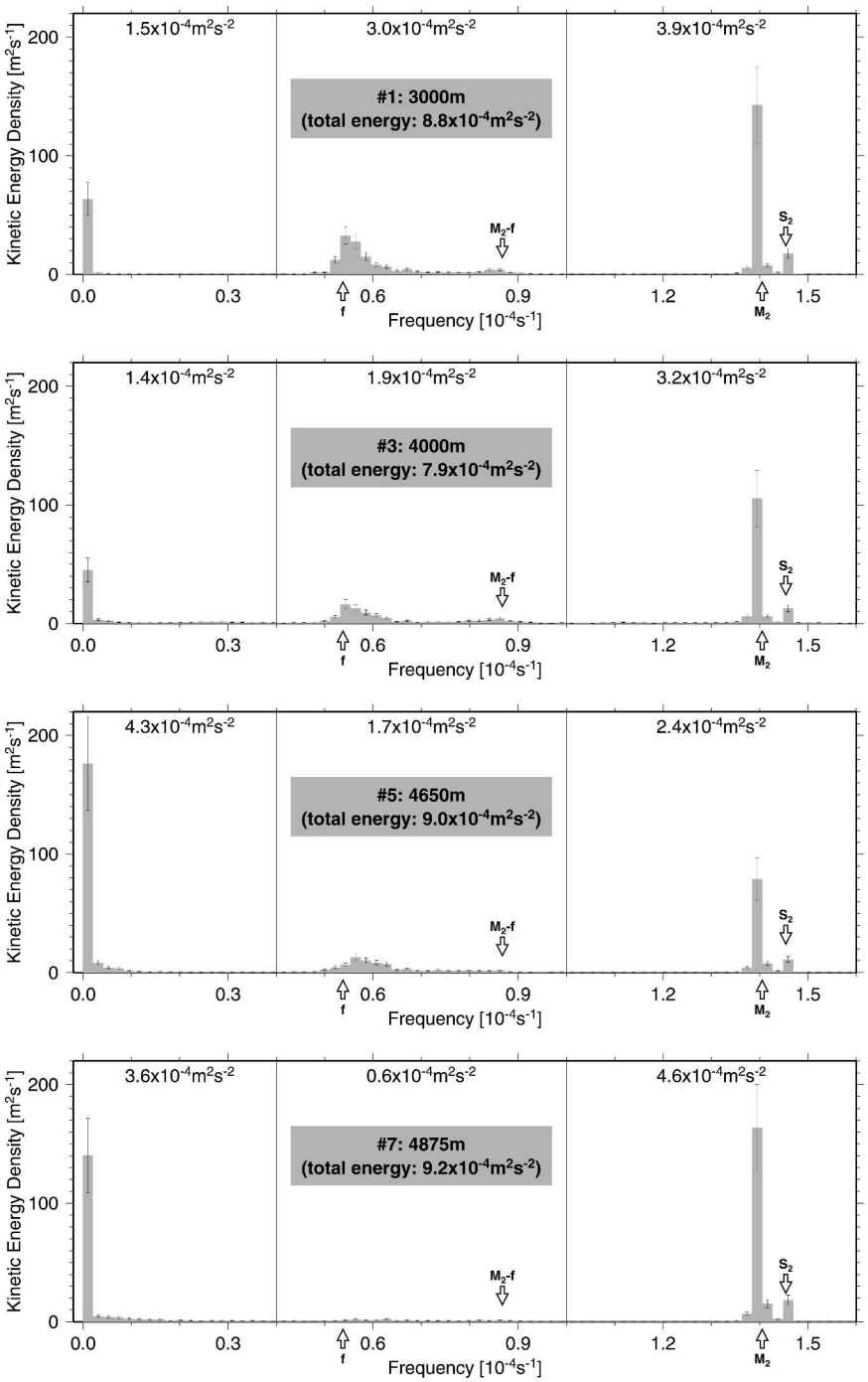

FIG. 4. Spectra of kinetic energy per unit mass (i.e., the integrated spectral energy densities equal one-half of the sums of the single-component velocity variances) for frequencies up to 2.2 cpd. Arrows point to the inertial band (f), semidiurnal tidal frequencies (M_2 and S_2), and a semidiurnal–inertial interaction frequency ($M_2 - f$). Each spectrum is derived from 2^{15} half-hourly measurements (683 days). Error bars show std devs based on averaging of 20 adjacent frequency bins. The numbers near the top of each panel give integrated spectral power in the frequency bands separated by vertical lines; the total kinetic energies (including the high frequencies, which are not shown) are listed in the gray boxes, below the instrument numbers and depths.

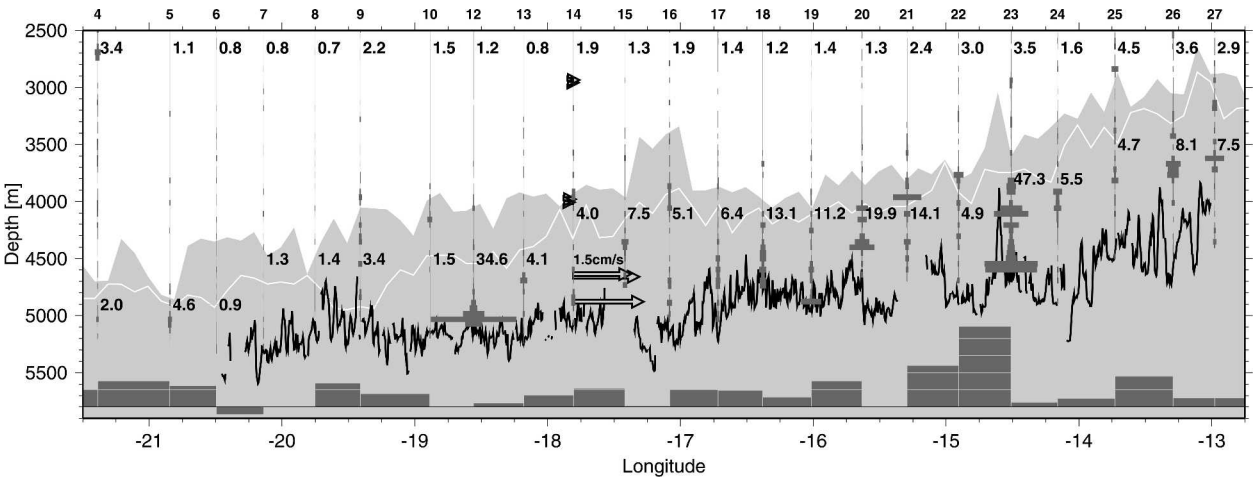

FIG. 5. Dissipation profiles (station numbers above the panel), along-canyon record-mean current-meter velocities (arrows near 17°45′W), and horizontal density gradients above the blocking topography (blocks below the valley floor) in the ridge-flank canyon; see Fig. 1 for regional setting. The jagged solid line shows the axial depth of the canyon between the dissipation stations where high-resolution multibeam data are available. The canyon-wall bathymetry (from Smith and Sandwell 1997) is shaded up to the peak of the higher of the two lateral walls; the white line shows the level of the lower wall. The 50-dbar-averaged dissipation profiles are displayed as horizontal bars; the peak value at station 12 is 3.2×10^{-8} W kg^{-1}. Depth-averaged dissipations between 2000 m and the mean depth of the two canyon walls are printed next to the profiles near 2700 m in units of 10^{-10} W kg^{-1}; the numbers printed inside the canyon correspond to the mean dissipations below the canyon-wall crests. Each density-gradient block represents a value of 10^{-7} kg m^{-3} m^{-1}, twice the temporal variability (see text); blocks above the zero line (at 5800 m) indicate eastward-decreasing densities.

with significantly different along-valley density gradients. One such region, between stations 7 and 9, is shown in Fig. 7. Again, there is an apparent correspondence between the presence of sills (between stations 8 and 9 but much less so between stations 7 and 8) and the magnitudes of the horizontal density gradients (1.4×10^{-7} kg m^{-3} m^{-1} between stations 8 and 9 and zero between stations 7 and 8; Fig. 5).

To test the hypothesis that the magnitudes of the horizontal density gradients in the canyon are related to the incidence of sills, the topographic variance between each station pair was separated into the contribution due to topographic peaks (variance above the median depth) and the contribution due to depressions (variance below the median depth). The result supports the hypothesis (Fig. 8): There is a strong association between the density gradients and the incidence of sills while there is no apparent relationship between the density gradients and the incidence of depressions. When the station pair with the highest density gradient

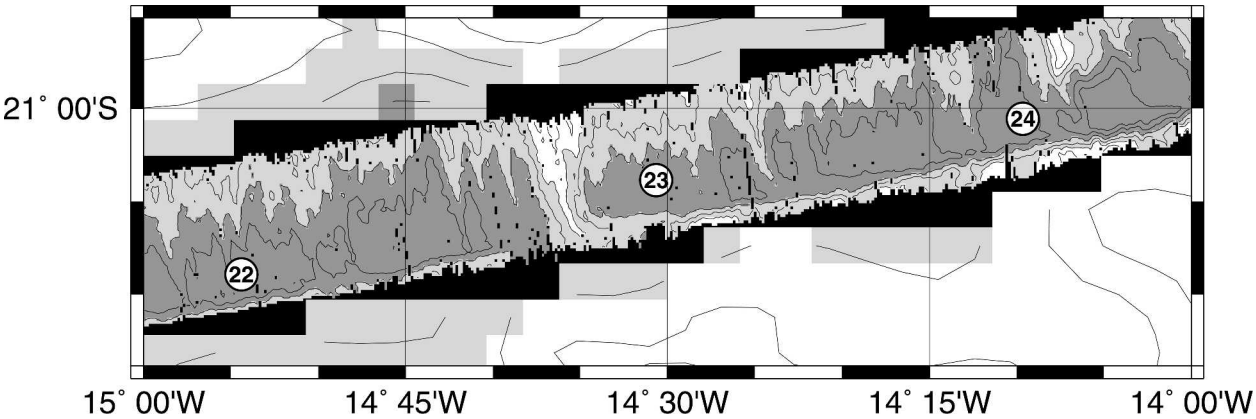

FIG. 6. Topography between stations 22 and 24, where the highest dissipation and the steepest along-axial density gradient in the canyon were observed (Fig. 5). Multibeam data are inset into the coarse-resolution topographic context (from Smith and Sandwell 1997) in order to show the lateral canyon walls; depths below 4000 are shaded; dark gray is used below 4500 m; contour interval is 250 m.

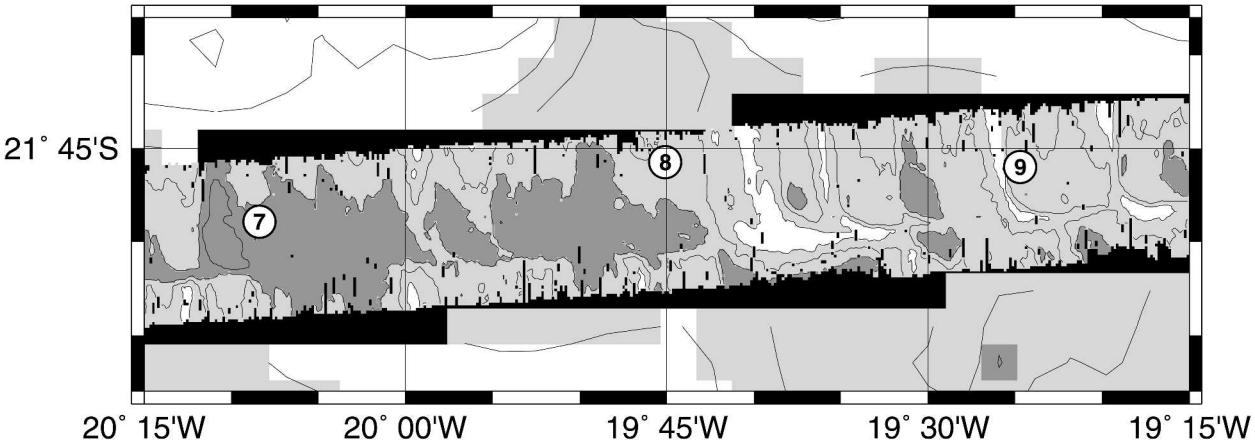

FIG. 7. Topography between stations 7 and 9. Depths below 5000 are shaded; dark gray is used below 5500 m; contour interval is 250 m.

is removed from the dataset, the correlation coefficient is reduced from $r = 0.8$ to 0.4, but the regression still passes the goodness-of-fit test (Q actually increases from 0.4 to 0.6). We note that topographic blocking cannot account for these observations because the density gradients are calculated at the levels of the sill depths between stations.

4. Discussion

a. Hydrography, flow, and mixing in canyons

The main result of our analysis of the hydrography, flow, and mixing in a canyon on the flank of the MAR in the South Atlantic is the observation of a strong association between along-axial horizontal density gradients and the incidence of cross-canyon sills. Assuming (approximately) constant transport along the canyon, this implies that the diapycnal buoyancy fluxes take place preferentially in the vicinity of sills. The association of mixing and sills is consistent with observations from other regions where cross-sill flows are also associated with high levels of diapycnal mixing (e.g., Wesson and Gregg 1994; Polzin et al. 1996; Thurnherr et al. 2002). The main candidate processes that can account for elevated mixing in the vicinity of sills—shear instability (e.g., Wesson and Gregg 1994), hydraulic jumps (e.g., Polzin et al. 1996), and topographic lee waves (e.g., Thurnherr and Richards 2001)—are not expected to be associated to the same degree with flow over depressions, consistent with our observations.

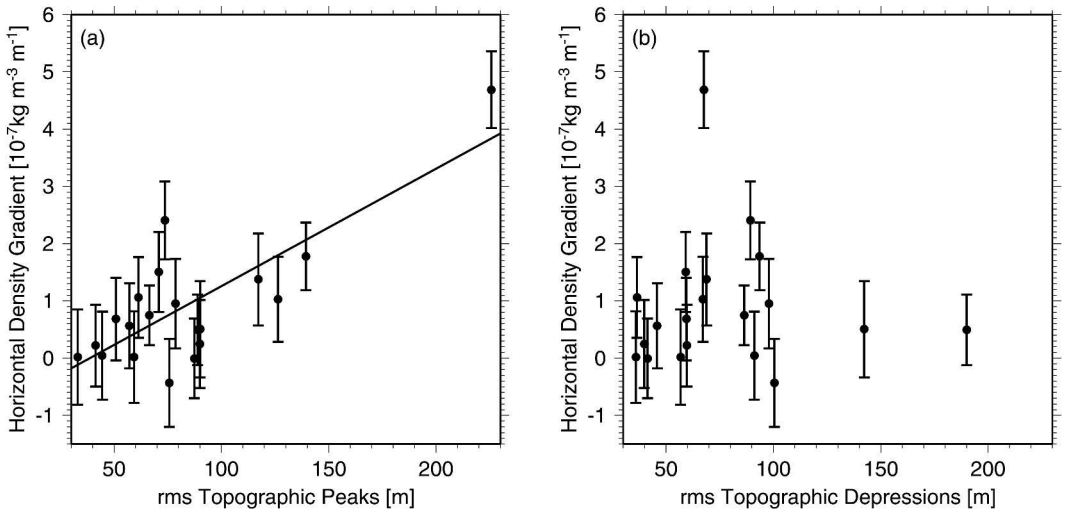

FIG. 8. Horizontal density gradients vs bathymetric roughness. (a) Influence of sills, defined as the topographic variance above the median depth along a straight line connecting two stations; the correlation coefficient r of the linear regression is 0.8, with a goodness-of-fit Q of 0.4. (b) Influence of depressions, defined as the topographic variance below the median depth between stations; the data are uncorrelated ($Q < 10^{-4}$).

It will be noted that our inferences about the mixing on the flank of the MAR in the Brazil Basin are different from the conclusions of previous studies. Polzin et al. (1997) and Ledwell et al. (2000) suggested that the enhanced dissipation in the eastern Brazil Basin is caused by breaking internal waves forced by the tides. However, the available microstructure data indicate that the majority of the dissipation in this region occurs inside the canyons rather than above the ridge-flank topography, and the current-meter records furthermore show that in one particular canyon there is at least as much low-frequency energy as tidal energy available for mixing. Therefore, breaking internal waves forced by the tides may well not be the dominant mechanism for mixing in the Brazil Basin, particularly inside the canyons. [The spring–neap modulation of the observed dissipation data (Ledwell et al. 2000; St. Laurent et al. 2001) is not inconsistent with sill-related mixing either, because tidal flows can modulate hydraulic processes (Helfrich 1995).]

The energy source for the observed low-frequency flow in the canyon is unclear. One possibility is that it is driven by mixing. A fraction (usually taken to be ≈20%) of the kinetic energy of externally imposed turbulence—for example, that associated with instability of tidal and/or inertial currents, acts to increase the potential energy of the water column, while the remainder is dissipated. In a sloping valley this potential energy made available by mixing can drive a (restratifying) up-valley flow. Another possible mechanism for enhancing subinertial flows in canyons is suggested by the results from a simple analytical and numerical model that shows how basin/sill combinations act as efficient low-pass filters of externally imposed mesoscale motions (Thurnherr 2000). Regardless of the ultimate cause of the low-frequency flow up the canyon, the along-canyon pressure gradient must be balanced somehow. While we are not yet able to answer this question it is noted that hydraulically controlled flows across sills are associated with greatly increased form drag (e.g., Moum and Nash 2000).

Sloping submarine valleys or canyons are not restricted to midocean ridge flanks. Canyons cutting across continental slopes and shelves in particular are found along many continental margins, and some have been extensively studied, not least because of their potential to affect biological productivity by increasing shelf-slope exchange of nutrients (e.g., Hickey 1995). Similar to the ridge-flank canyons, shelf-slope canyons can also be associated with enhanced levels of diapycnal mixing (e.g., Carter and Gregg 2002), which is usually attributed to the trapping of internal-wave energy (in particular in the semidiurnal tidal band) by the steep canyon walls (Gordon and Marshall 1976; Hotchkiss and Wunsch 1982). [In contrast, the lateral walls of the ridge-flank canyons in the Brazil Basin are not deep enough to trap the semidiurnal internal tides (Polzin 2004).] Low-frequency along-canyon flows are also commonly observed in shelf-slope canyons, where they are usually inferred to be driven by externally imposed along-axial pressure gradients related to wind forcing or to along-shelf (i.e., cross-canyon) currents in the overlying water column (e.g., Hickey 1995). However, Cannon (1972) describes an asymmetry in the response of the flow field in a canyon to the wind, and attributes it to an upwelling-favorable along-axial density gradient of unexplained origin. Similarly, Hunkins (1988) reports up-canyon mean flow in the lower part of a different shelf-slope canyon, which underlies downwelling-favorable along-shelf flow.

b. *Mixing in canyons versus mixing above the topography*

To compare the relative importance of mixing in canyons and mixing above the rough ridge-flank topography, a buoyancy budget for the AABW–NADW interface in the Brazil Basin was constructed (Table 1). Outside the ridge-flank canyons the interface was assumed to coincide with the 3500-m isobath, the approximate mean depth of the 2°C potential isotherm. The interfacial area was separated into three topographic classes: above the smooth abyssal plain, inside canyons, and above the ridge-flank topography (i.e., above the canyons and canyon walls). The areal contributions of the different classes were estimated from geometric considerations: The mean zonal width of the Brazil Basin at 3500 m is ≈2000 km. Using a ridge-flank slope of 1–2 × 10^{-3} and a canyon depth of 500–1000 m (Thurnherr and Speer 2003) yields an estimate of 500 km for the zonal excursions of isobaths into the canyons. Noting the horizontal density decrease toward the MAR crest in the canyons, the zonal excursions of isopycnal surfaces into the canyons are <500 km and we estimate that 15% of the isopycnal surface separating AABW from

TABLE 1. Relative contributions of three topographic classes to the buoyancy flux across the NADW–AABW interface in the Brazil Basin; mean dissipations outside canyons were averaged below 2000 m; areal contributions were estimated from the basin geometry.

Region	Area	Mean dissipation	Buoyancy-flux contribution
Above abyssal plain	40%	0.9×10^{-10} W kg^{-1}	14%
Inside canyons	15%	9.3×10^{-10} W kg^{-1}	53%
Above MAR flank	45%	1.9×10^{-10} W kg^{-1}	33%

NADW lie inside canyons. The observed dissipation on the rough flank of the MAR is nearly 5 times as large inside the canyon analyzed here than above the topography, while the mean dissipation above the smooth abyssal plain west of 28°W (in the data analyzed by Polzin et al. 1997) is an order of magnitude smaller than the dissipation in the canyon. Making the usual assumption of a constant mixing efficiency, diapycnal mixing in the ridge-flank canyons accounts for approximately one-half of the total buoyancy flux, while about one-third is due to mixing above the ridge-flank topography.

The heat-budget-derived up-canyon velocity calculated by St. Laurent et al. (2001) is 1/4–1/6 of the mean up-canyon velocities recorded by the current meters. While we cannot exclude the possibility that this apparent discrepancy is due to temporal and/or spatial variability in the flow field, it is also possible that the available dissipation data are biased low. Because of tracer-sampling considerations, the microstructure profiles in the canyon were taken in topographic depressions away from the immediate vicinity of sills. Together with the observed association between sills and along-axial density gradients this suggests that the high-mixing regions have been undersampled, implying that the relative buoyancy-flux contribution of canyons to the AABW-NADW buoyancy budget may be even greater than estimated above.

Additional support for the hypothesis that the high-mixing regions in the canyon may have been undersampled is provided by the following argument: Sills locally reduce the cross-sectional area of the canyon. To conserve transport, the along-canyon flow is expected to accelerate over the sills, which by implication, increases the associated vertical shear. Lacking velocity observations from a sill in the canyon analyzed here, this effect cannot be assessed directly but it is noted that the sill near 14°30′W blocks more than 50% of the cross-sectional area of the canyon. Strong acceleration of along-canyon flow over a sill has been observed elsewhere: Between 1997 and 1998 the velocity field in the vicinity of a 800-m-high sill connecting two rift-valley segments near 36°N was monitored by 21 current meters on 7 moorings (Thurnherr et al. 2002). The topographic and hydrographic characteristics of the rift valley are similar to the ridge-flank canyon studied here, and the spectral energy levels observed away from the immediate proximity of the sill (30 km downstream) in the rift valley are nearly identical to the levels inferred from the ridge-flank canyon current meters (Table 2). On the saddle of the rift-valley sill, the low-frequency energy is enhanced by more than an order of magnitude. If the along-axial flow in the ridge-flank canyon analyzed here is similarly enhanced on the sills, the high-shear and -mixing regions associated with sills have not been sampled at all.

c. Global significance

Thurnherr and Speer (2003) show that most of the canyons on both flanks of the MAR in the South Atlantic are associated with similar along-axial density gradients, and that these gradients can be maintained by a balance of horizontal advection toward the ridge crest and vertical eddy diffusion. Inspection of global topographic maps reveals that deep cross-flank canyons are associated with all slow-spreading midocean ridges, which make up 2/3 of the 40 000-km-long global ridge system. The first- and second-order segmentation of slow-spreading ridges, which gives rise to the cross-flank canyons, is associated with an along-axial spacing of 50 ± 30 km (Tucholke and Lin 1994). Therefore,

TABLE 2. Topographic and hydrographic characteristics, as well as current-meter derived kinetic energies (KE), in the ridge-flank canyon analyzed here and in two connected rift-valley segments investigated by Thurnherr et al. (2002). The axial slope of the rift valley was estimated from the saddle depths of the inflow and outflow sills. The mean ridge-flank canyon diffusivity was derived from dissipation measurements and has been used in the heat budget of St. Laurent et al. (2001). The rift-valley diffusivity was derived from heat and salt budgets (Thurnherr et al. 2002). The kinetic-energy estimates were calculated from the records of current meters moored 300–500 m above the seabed.

Property	Ridge-flank canyon	Rift valley
Width	20–40 km	10–30 km
Depth (h)	500–1000 m	500–1000 m
Along-canyon slope	0.7×10^{-3}	$0.5–1 \times 10^{-3}$
Buoyancy frequency (N)	$0.2–1 \times 10^{-3}$ s^{-1}	$0.2–1 \times 10^{-3}$ s^{-1}
Deformation radius (Nh/f)	2–20 km	1–12 km
Along-canyon density gradient	10^{-7} kg m^{-3} m^{-1}	10^{-7} kg m^{-3} m^{-1}
Bulk diffusivity	4×10^{-3} m^2 s^{-1}	$3–8 \times 10^{-3}$ m^2 s^{-1}
"Off-sill" tidal + inertial KE	4.1×10^{-4} m^2 s^{-2}	4.0×10^{-4} m^2 s^{-2}
"On-sill" tidal + inertial KE	Unknown	7.1×10^{-4} m^2 s^{-2}
"Off-sill" subinertial KE	4.3×10^{-4} m^2 s^{-2}	4.2×10^{-4} m^2 s^{-2}
"On-sill" subinertial KE	Unknown	43.2×10^{-4} m^2 s^{-2}

there are approximately 1000 cross-flank canyons globally, counting the ridge flanks separately. The ubiquity of abyssal hills, which are aligned parallel to the spreading axes of midocean ridges (e.g., Goff et al. 1995), implies that cross-canyon sills are common. A visual survey of the canyon studied here indicates that there are 10–15 sills rising at least 250 m above the canyon floor between 13° and 17°W. If this number is globally representative, and if it is furthermore assumed that there are significant low-frequency flows along the axes of a substantial fraction of the ridge-flank canyons, there are $O(10^4)$ overflows in ridge-flank canyons in the deep ocean.

The question of which processes are responsible for the enhanced mixing on the MAR flank in the South Atlantic is important. Several recent mixing parameterizations that are based on the Brazil Basin observations ignore the presence of canyons and sills. If processes associated with flows across sills contribute significantly to the mixing, these parameterizations cannot be expected to be accurate, especially in regions with different topographic characteristics. We note that the fast-spreading ridges in the Pacific Ocean are morphologically very different from the MAR and we expect the parameterizations based on the Brazil Basin measurements to be particularly inappropriate there. Resolution of the issues raised in this study requires further investigation, ideally involving laboratory and numerical experiments as well as additional targeted fine and microstructure surveys.

Acknowledgments. We thank Kurt Polzin for helpful criticism of an earlier version of this manuscript. Data collection and analysis have been supported by the National Research Foundation through Grants OCE-9415589 and OCE-9415598 for field work, and OCE-0220407 (AMT), OCE-9906685 (JRL), OCE-0217075 (JMT) for analysis.

REFERENCES

Cannon, G. A., 1972: Wind effects on currents observed in Juan de Fuca submarine canyon. *J. Phys. Oceanogr.,* **2,** 281–285.

Carter, G. S., and M. C. Gregg, 2002: Intense, variable mixing near the head of Monterey submarine canyon. *J. Phys. Oceanogr.,* **32,** 3145–3165.

Goff, J. A., B. E. Tucholke, J. Lin, and G. E. Jaroslow, 1995: Quantitative analysis of abyssal hills in the Atlantic Ocean: A correlation between inferred crustal thickness and extensional faulting. *J. Geophys. Res.,* **100,** 22 509–22 522.

Gordon, R. L., and N. F. Marshall, 1976: Submarine canyons: Internal wave traps? *Geophys. Res. Lett.,* **3,** 622–624.

Helfrich, K. R., 1995: Time-dependent two-layer hydraulic exchange flows. *J. Phys. Oceanogr.,* **25,** 359–373.

Hickey, B. M., 1995: Coastal submarine canyons. *Flow Topography Interactions: 'Aha Huliko'a Winter Workshop,* University of Hawaii at Manoa, 95–110.

Hogg, N., P. Biscaye, W. Gardner, and W. J. Schmitz, 1982: On the transport and modification of Antarctic Bottom Water in the Vema Channel. *J. Mar. Res.,* **40,** 231–263.

Hotchkiss, F. S., and C. Wunsch, 1982: Internal waves in Hudson Canyon with possible geological implications. *Deep-Sea Res.,* **29A,** 415–442.

Huang, R. X., and X. Jin, 2002: Deep circulation in the South Atlantic induced by bottom-intensified mixing over the midocean ridge. *J. Phys. Oceanogr.,* **32,** 1150–1164.

Hunkins, K., 1988: Mean and tidal currents in Baltimore Canyon. *J. Geophys. Res.,* **93,** 6917–6929.

Ledwell, J. R., E. T. Montgomery, K. L. Polzin, L. C. St. Laurent, R. W. Schmitt, and J. M. Toole, 2000: Evidence for enhanced mixing over rough topography in the abyssal ocean. *Nature,* **403,** 179–182.

Morris, M. Y., M. M. Hall, L. C. St. Laurent, and N. G. Hogg, 2001: Abyssal mixing in the Brazil Basin. *J. Phys. Oceanogr.,* **31,** 3331–3348.

Moum, J. N., and J. D. Nash, 2000: Topographically induced drag and mixing at a small bank on the continental shelf. *J. Phys. Oceanogr.,* **30,** 2049–2054.

Müller, R. D., W. R. Roest, J.-Y. Royer, L. M. Gahagan, and J. G. Sclater, 1997: Digital isochrons of the world's ocean floor. *J. Geophys. Res.,* **102,** 3211–3214.

Polzin, K., 2004: Idealized solutions for the energy balance of the finescale internal wave field. *J. Phys. Oceanogr.,* **34,** 221–246.

——, K. G. Speer, J. M. Toole, and R. W. Schmitt, 1996: Intense mixing of Antarctic Bottom Water in the equatorial Atlantic Ocean. *Nature,* **380,** 54–57.

——, J. M. Toole, J. R. Ledwell, and R. W. Schmitt, 1997: Spatial variability of turbulent mixing in the abyssal ocean. *Science,* **276,** 93–96.

Simmons, H. L., S. R. Jayne, L. C. St. Laurent, and A. J. Weaver, 2004: Tidally driven mixing in a numerical model of the ocean general circulation. *Ocean Modell.,* **6,** 245–263.

Smith, W. H. F., and D. T. Sandwell, 1997: Global seafloor topography from satellite altimetry and ship depth soundings. *Science,* **277,** 1956–1962.

St. Laurent, L. C., J. M. Toole, and R. W. Schmitt, 2001: Buoyancy forcing by turbulence above rough topography in the abyssal Brazil Basin. *J. Phys. Oceanogr.,* **31,** 3476–3495.

——, H. L. Simmons, and S. R. Jayne, 2002: Estimating tidally driven mixing in the deep ocean. *Geophys. Res. Lett.,* **29,** 2106, doi:10.1029/2002GL015633.

Thurnherr, A. M., 2000: Hydrography and flow in the rift valley of the Mid-Atlantic Ridge. Ph.D. thesis, School of Ocean and Earth Science, University of Southampton, Southampton, United Kingdom, 156 pp.

——, and K. J. Richards, 2001: Hydrography and high-temperature heat flux of the Rainbow hydrothermal site (36°14′N, Mid-Atlantic Ridge). *J. Geophys. Res.,* **106,** 9411–9426.

——, and K. G. Speer, 2003: Boundary mixing and topographic blocking on the Mid-Atlantic Ridge in the South Atlantic. *J. Phys. Oceanogr.,* **33,** 848–862.

——, K. J. Richards, C. R. German, G. F. Lane-Serff, and K. G. Speer, 2002: Flow and mixing in the rift valley of the Mid-Atlantic Ridge. *J. Phys. Oceanogr.,* **32,** 1763–1778.

Tucholke, B. E., and J. Lin, 1994: A geological model of the structure of ridge segments in the slow spreading ocean crust. *J. Geophys. Res.,* **99,** 11 937–11 958.

Wesson, J. C., and M. C. Gregg, 1994: Mixing at Camarinal Sill in the Strait of Gibraltar. *J. Geophys. Res.,* **99,** 9847–9878.